Engineering Fracture Mechanics Vol. 42, No. 3, pp. 519–530, 1992
Printed in Great Britain.

0013-7944/92 $5.00 + 0.00

SPOT WELD FAILURE FROM BUCKLING-INDUCED STRESSING OF BEAMS UNDER CYCLIC BENDING AND TORSION

G. A. KARDOMATEAS
School of Aerospace Engineering, Georgia Institute of Technology, Atlanta, GA 30332-0150, U.S.A.

Abstract—An important design constraint of spot-welded beams is the fatigue strength of the spot welds. The present study is concerned with predicting the cyclic life of the spot-welded joints in beams under bending and torsion. First the physical mechanism of buckling-induced stressing is analyzed. The stress distribution is obtained from a two-dimensional buckling model. Afterwards, an expression for the J integral is found in terms of the geometric and loading parameters. This expression is used with a Paris' law type of fatigue crack growth to assess the fatigue life of the design. Subsequently, an analysis that explains the phenomenon for the case of torsion loading is provided. An example case is treated in order to obtain numerical results for the J integral and the number of fatigue cycles as a function of the applied loading or the weld spacing.

INTRODUCTION

SPOT-WELDED thin steel beams exist in the body of vehicles and constitute the major load carrying members. The needs of an optimized construction call for an ability to predict the strength and durability of body structures with higher accuracy at the early stages of design. This, in turn, calls for a means to accurately evaluate the strength of spot-welded configurations and understand the physical variables that affect the durability.

A similar configuration occurs in aerospace structures, namely in compression panels with skin attached by rivets. The common feature is the spacing of the joints (spot welds or rivets). Examples of such structures are: skin-stringer wing surfaces, fuselage stringers, and shells supporting rings. In all cases the critical event is the buckling of the beam or flange between the spot welds or the buckling of the skin between the rivets.

In recent years there has been a considerable amount of work directed toward understanding the factors controlling the fatigue resistance of spot-welded sheets [1–5]. Most studies have concentrated on the investigation of the strength of joints under applied tension which causes shearing of the spot welds [2–5].

The typical structural element under consideration is the box section single or double hat beam (Figs 1 and 2), which consists of a hat section with its flanges spot-welded to a closing plate. The mechanism of fatigue fracture and the deformation pattern occurring in such configurations is different from the fatigue of a single spot-welded joint under tensile or shearing load. This is because the inherent imperfection and waviness at the segments between spot welds leads to buckling deflections under bending or compressive loading. The repeated stressing from these displacements may lead to fatigue failure of the welds. The present study is concerned with such cases of buckling-induced failure of spot welds. The problem is investigated by means of a buckling analysis and a closed form expression for the J integral at the spot weld site is derived. The objective is to develop simple methodologies suitable for preliminary design which can serve as the means for selecting and screening candidate configurations, isolating the parameters that control the fatigue behavior and providing trend information.

BUCKLING MODEL

We will model the opening of the spot-welded flange. This model is similar to the one described in ref. [1]. As shown in Fig. 3, assume a spot weld spacing l and an initial deflection $y_0(x)$ (due to an inherent waviness in the initial shape of the flange). The segment between the spot welds is, therefore, a beam with both ends assumed fixed at the weld sites. An axial compression P and an end moment M, constitute the loading. We shall discuss the source of the loading at a later stage.

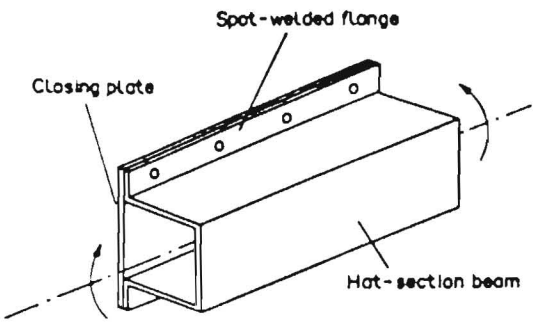

Fig. 1. Spot weld box beam.

The form of the initial deflection $y_0(x)$ is obviously dependent upon the material, the dimensions and the welding conditions of the beam; however, for the purposes of analytical treatment, we can take y_0 as a trigonometric function with deflection at the middle, v_0:

$$y_0(x) = \frac{v_0}{2}\left(1 - \cos\frac{2\pi}{l}x\right). \tag{1}$$

Denote by $y_1(x)$ the additional deflection caused by the loading, then the differential equation for the deflection of the beam is (Fig. 3):

$$EI_p \frac{d^2 y_1(x)}{dx^2} = -P[y_1(x) + y_0(x)] + M_A. \tag{2}$$

where E is the modulus of elasticity and I_p is the moment of inertia of the part being modeled (i.e. the flange or the closing plate): $I_p = w_f t^3/12$ where t is the thickness of the sheet metal and w_f is the flange width.

To solve (2) set

$$y_1(x) = \frac{v_1}{2}\left(1 - \cos\frac{2\pi}{l}x\right), \tag{3}$$

and substitute in (2). In terms of

$$P_{cr} = \frac{4\pi^2 EI_p}{l^2} \tag{4}$$

we obtain the following by equating the constant terms and the coefficients of $\cos(2\pi x/l)$:

$$v_1 = \frac{v_0 P}{P_{cr} - P}, \tag{5a}$$

$$M_A = \frac{P}{2}(v_1 + v_0) = v_0 P \frac{P_{cr}}{2(P_{cr} - P)}. \tag{5b}$$

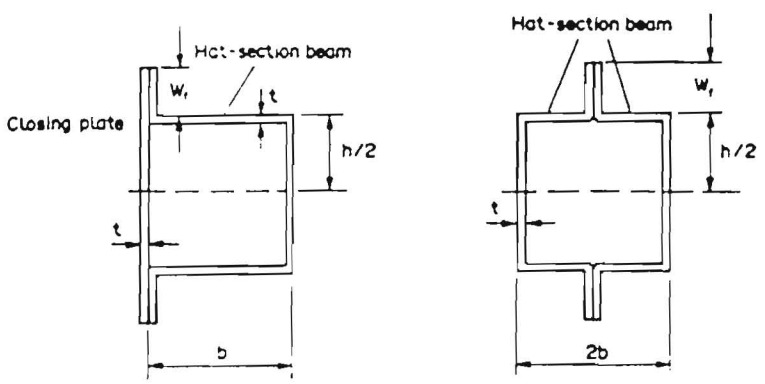

Fig. 2. Single hat and double hat section box beam.

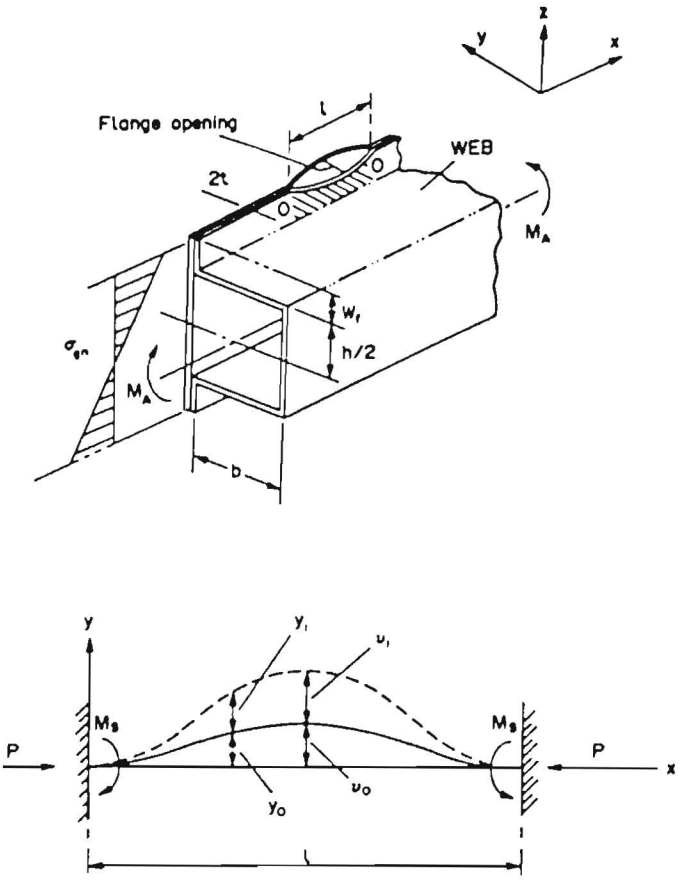

Fig. 3. Buckling model for the spot weld spacing on the flange.

The total maximum deflection, midway between the spot welds, is

$$f = v_0 + v_1 = v_0 \frac{P_{cr}}{P_{cr} - P}, \tag{6}$$

i.e. it is proportional to the maximum initial deflection v_0 and has a nonlinear relationship with the compressive force P.

For the two thin metal sheets with spot welds, subjected to axial compression $2P$, the above relations describe the deformation pattern due to the buckling of the segments between the spot welds. However, for the usual hat section cross-sectional geometry, subjected to a bending moment M_A, we need relations for the resultant axial force P and the moment of inertia. To determine the resultant compressive force we integrate the bending stress over the flange width w_f (Fig. 3):

$$P = \int_{h/2}^{(h/2)+w_f} t \frac{M_A}{I_b} z \, dz = t \frac{M_A}{2I_b}(hw_f + w_f^2), \tag{7}$$

where the moment of inertia for the whole beam is given as follows (Fig. 2):

$$I_b = 2(bt)\left(\frac{h}{2}\right)^2 + \frac{th^3}{12} + \frac{t(h + 2w_f)^3}{12} + \frac{tw_f}{6}[w_f^2 + 3(h + w_f)^2]. \tag{8}$$

Before we proceed to the evaluation of the J integral for the geometry of our problem, we shall discuss another subject of importance. In being deflected in the buckling mode, the flange is elastically restrained by the web of the hat section beam. The closing plate is in turn restrained as shown in Fig. 4. The effect of the restraint is to increase the buckling load. To assess this effect we should solve the problem of buckling of a plate with both left and right sides clamped and the

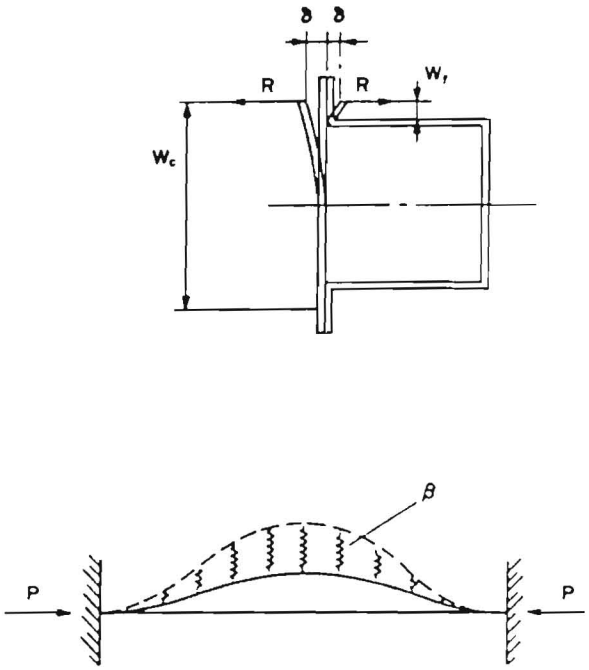

Fig. 4. Model of the elastic restraint of the flange by the web.

lower edge also being clamped. For the purposes of this study we shall use a simpler approach considering that the restraint is a spring [1]. Since for a load R (along the x-axis) the deflection of a clamped beam of length b and moment of inertia I is

$$\delta = \frac{Rw^3}{3EI}, \tag{9a}$$

the spring constant per unit length is

$$\beta = \frac{R}{\delta} = \frac{3EI}{w^3} = \frac{Et^3}{4w^3}, \tag{9b}$$

where w is the width of either the flange (w_f) or the closing plate (w_c) as shown in Fig. 4. Then we can say we have a beam on an elastic foundation of modulus β per unit length. The buckling load in such a case (Fig. 4) is given by [6]

$$P_{cr} = \frac{4\pi^2 EI_p}{l^2}\left(m^2 + \frac{3\beta l^4}{4m^2\pi^4 EI_p}\right). \tag{10}$$

where m is an integer. Thus the critical load is given as a function of m, which represents the number of half cosine waves in which the bar subdivides at buckling. The lowest critical value may occur with $m = 1$ or a higher value depending on the values of the other constants. It can be seen that since β is larger for the flange, the critical load P_{cr} on the closing plate is less than the corresponding one for the hat section beam. This means that buckling occurs more easily on the closing plate side. Moreover, m would typically be larger than unity for the flange, so that the buckled shape of the hat section would have more than one half cosine wave shape.

The double hat section beam consists of hat section beams with no closing plate (Fig. 2). For this geometry

$$I_b = 2\left\{2(bt)\left(\frac{h}{2}\right)^2 + \frac{th^3}{12} + \frac{tw_f}{6}[w_f^2 + 3(h + w_f)^2]\right\}. \tag{11}$$

J INTEGRAL

For two-dimensional problems of materials governed by nonlinear elasticity and deformation plasticity theory, the J integral is defined as [7]

$$J = \int_\Gamma W\,dy - \mathbf{T}\cdot\frac{\partial \mathbf{u}}{\partial x}\,ds, \tag{12}$$

where Γ = contour surrounding the crack tip, $\mathbf{T}$ = traction vector along the contour, $\mathbf{u}$ = displacement vector on the contour, and W = strain energy density on the contour. The coordinate system is such that the x-axis is parallel to the crack faces and the integral is evaluated in a contraclockwise sense.

A cross-section of the beam ahead of the spot weld carries a compressive load $2P$. Behind the spot weld the two cross-sections of the buckled configuration below and above the spot weld carry load P and bending moment M. To evaluate the J integral we decompose the system of loads in Fig. 5a into two subsystems as shown in Fig. 5b,c. The first subsystem consists only of moment loading behind the spot weld (no loading ahead of the spot weld) and the second subsystem consists of the axial loading both behind and ahead of the spot weld (Fig. 5c). The second subsystem produces a nonsingular stress field of pure compression near the spot weld front,

$$\sigma_{11} = -2P/(2t), \tag{13}$$

and therefore the mode I and II stress intensity factors associated with this subsystem of loading vanish. Consequently, the stress intensity factors and J integral values or energy release rate values associated with the total loading system are the same as those associated with the first subsystem of loading.

Consider a line-integration contour as shown in Fig. 5b, with the segment of the flange between the spot welds being in the buckled state as described before. Only the segment 34 contributes to the J integral since the rest of the cross-section ahead of the spot weld is subjected to vanishing stress and strain. Assume $\sigma_{11} = \tau_{11} = \tau_{12} = \tau_{13} = 0$. Along the vertical segment 34 the strain energy is

$$W = \int_0^{\varepsilon_{11}} \sigma_{11}\,d\varepsilon_{11} = \tfrac{1}{2}(\sigma_{11}\varepsilon_{11} + \sigma_{22}\varepsilon_{22}). \tag{14}$$

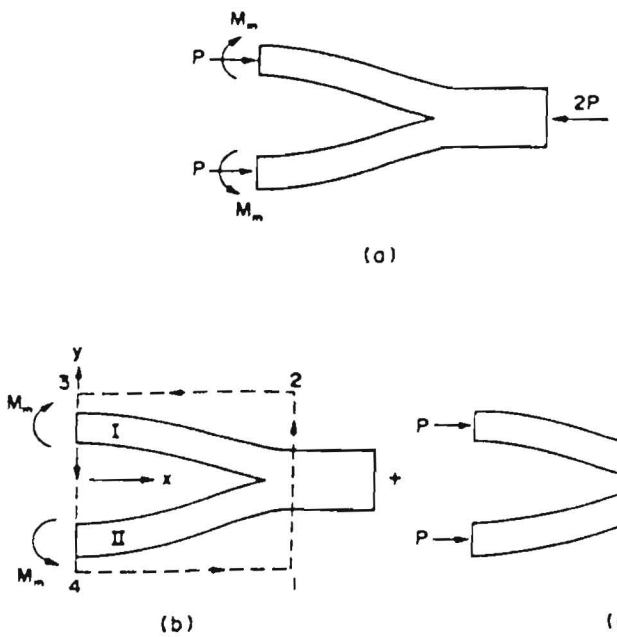

Fig. 5. Contour for the calculation of the J integral.

Furthermore, assume $\epsilon_{zz} = 0$ since the dimension in the z-direction is large. Then from

$$\epsilon_{zz} = \frac{1}{E}[\sigma_{zz} - \nu(\sigma_{xx} + \sigma_{yy})] \tag{15a}$$

we conclude that

$$\sigma_{zz} = \nu\sigma_{xx}, \tag{15b}$$

where ν is Poisson's ratio. Also, we find

$$\epsilon_{xx} = \frac{1}{E}(\sigma_{xx} - \nu\sigma_{zz}) = (1 - \nu^2)\frac{\sigma_{xx}}{E}. \tag{16}$$

Therefore,

$$W = \frac{1}{2E}(1 - \nu^2)\sigma_{xx}^2. \tag{17}$$

Now along 34 we have as the only component of the traction vector $T_x = -\sigma_{xx}$ and for the corresponding component of the displacement vector derivative $\partial u_x/\partial x = \epsilon_{xx}$. Moreover, along 34 we have $dy = -ds$, so the integral in (12) becomes

$$J_{34} = \int_{34}(\sigma_{xx}\epsilon_{xx} - W)\,ds = \int_{34}\frac{(1 - \nu^2)}{2E}\sigma_{xx,m}^2\,ds, \tag{18}$$

where $\sigma_{xx,m}$ is the stress at the middle of the weld spacing.

Now we need expressions for the stress at the weld and at the middle of the spacing. The stress in the direction of the box beam axis midway between the spot-welded points is found in terms of the bending moment at that location:

$$M_m = M_1 = -EI_y y_1''(x)|_{x=l/2} = EI_y\frac{c}{2}\frac{4\pi^2}{l^2} = v_0 P\frac{P_{cr}}{2(P_{cr} - P)}. \tag{19}$$

We see that the moment midway between the spot welds is the same as that at the spot weld sites. The stress produced by the moment M at the cross-section above the spot weld line and midway between the spot welds is

$$\sigma_{xx,m}^{I}(s) = \frac{M_m s}{I_y}; \quad -t/2 \leq s \leq t/2. \tag{20a}$$

For the buckled part below the spot weld line

$$\sigma_{xx,m}^{II}(s) = -\frac{M_m s}{I_y}; \quad -t/2 \leq s \leq t/2, \tag{20b}$$

where t is the thickness of each metal sheet. Integrating we get

$$J = J_{34} = \frac{(1 - \nu^2)}{2E}\left(\int_{-t/2}^{t/2}\sigma_{xx,m}^{I}(s)\,ds + \int_{-t/2}^{t/2}\sigma_{xx,m}^{II}(s)\,ds\right) = \frac{(1 - \nu^2)}{E}\frac{M_1^2 t^3}{12I_y^2}. \tag{21}$$

The J integral depends on the weld spacing l through the expression of the moment M_1, eqs (19) and (21). Specifically, in terms of

$$c_1 = 4\pi^2 EI_y, \tag{22a}$$

we get

$$M_1 = v_0 P\frac{c_1}{2(c_1 - Pl^2)}. \tag{22b}$$

Set

$$c_1 = \frac{(1 - \nu^2)}{E}\frac{t^3}{48I_y^2}c_1^2. \tag{22c}$$

The J integral is now expressed in the following form:

$$J = P^2 v_0^2 \frac{c_2}{(c_1 - Pl^2)^2}. \tag{23}$$

FATIGUE ANALYSIS

On the basis of Paris' law [8], we have

$$\frac{da}{dN} = A(\Delta J)^n, \tag{24}$$

where a = the crack length, N = the number of cycles, A and n are constants of the material and ΔJ is the range of the J integral, which is taken from a value of load equal to zero to a range ΔP.

The crack in this case is the segment between the spot welds. Define $f(l, \Delta P)$ by

$$f(l, \Delta M_A \text{ or } \Delta P) = \Delta J = (\Delta P)^2 v_0^2 \frac{c_2}{[c_1 - (\Delta P) l^2]^2}. \tag{25}$$

Inserting we find

$$\frac{dl}{dN} = A f^n(l, \Delta P). \tag{26}$$

Separating and integrating for growth through the weld diameter d during the fatigue life N_f for a given loading range from zero to ΔP (or ΔM_A) we get

$$\int_l^{l+d} f^{-n}(l, \Delta P)\, dl = A \int_0^{N_f} dN. \tag{27}$$

Let

$$I(l, \Delta P) = \int_l^{l+d} f^{-n}(l, \Delta P)\, dl = \int_l^{l+d} \frac{1}{c_2^n} [c_1 - (\Delta P) l^{*2}]^{2n}\, dl^*. \tag{28}$$

This integral can be evaluated numerically for each application case. We get

$$(\Delta P)^{2n} v_0^{2n} N_f = \frac{I(l, \Delta P)}{A}. \tag{29}$$

So for a given spacing l and loading, the number of cycles can be calculated.

It should be pointed out that the above relation (26) is valid for

$$\Delta J_{th} < \Delta J < J_c, \tag{30}$$

where ΔJ_{th} is the threshold value and J_c is the critical fracture toughness value. Determination of threshold values through experimental means would be required since data for ΔJ_{th} are not easily available in the literature.

TORSION LOADING

In the usual presentation of torsion of thin walled sections, which is based on the elementary theory, the discussion is confined to the shearing stresses and the assumption that plane cross-sections remain plane. However, cross-sections do warp out of their original planes as the torque is applied. This warping is very important in the strength of the structure because restricting it gives rise to constraint forces at the flanges that can cause local opening of the segments between the spot welds [9]. We shall discuss this phenomenon in detail. First, we idealize the cross-section of the single or double hat member as a shell consisting of four corner flanges and idealized walls carrying only shear (Fig. 6). The four flanges are the only members capable of carrying longitudinal normal stresses.

Now assume that we apply an external torque T. Let us assume that the rectangular box shown in Fig. 6 twists through the angle ϕ in such a manner that the end bulkheads remain plane and

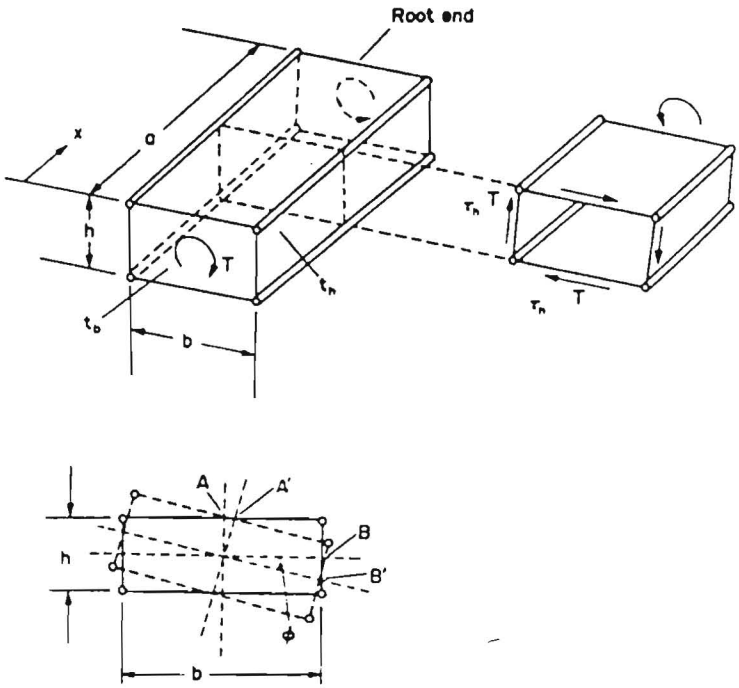

Fig. 6. Deformation produced by a twisting moment.

parallel to each other. The end bulkheads have width b and height h and the length of the box is a. The ratio of the shear strains produced by the twist can be found by considering the horizontal displacement of point A to A′ by the amount $\phi h/2$ and the vertical one of point B to B′ by the amount $\phi b/2$ (Fig. 6):

$$\gamma_h = \phi \frac{h}{2a}; \quad \gamma_h = \phi \frac{b}{2a}; \quad \frac{\gamma_b}{\gamma_h} = \frac{h}{b}. \tag{31}$$

The corresponding ratio of shear stresses from elementary torsion theory is:

$$\tau_b^T = \frac{T}{2bht_b}; \quad \tau_h^T = \frac{T}{2bht_h}; \quad \frac{\tau_b}{\tau_h} = \frac{t_h}{t_b}, \tag{32}$$

where t_b is the thickness of the top and bottom plates and t_h is the thickness of the side plates.

Since the shear strains multiplied by the shear modulus give the shear stresses, the two ratios in (31) and (32) should be the same. This occurs only in the special case $h/b = t_h/t_b$. Therefore, in addition to the twist, there is a second deformation in the unrestrained sections: the bulkheads, and indeed all the cross-sections, warp out of their original planes in an antisymmetric manner as shown in Fig. 7 and thus the shear strains in (31) are modified by an additional shear deformation of the walls until the final shear strains are compatible with the shear stresses determined by (32).

Now assume that we restrict the warping deformation. In the following we assume that the boxed shell is fixed rigidly at the root and free at the tip and it is subjected to a torque T (Fig. 8). Under these circumstances, at the tip there is no restraint or external axial force; this is not the case at the root. As was said earlier, a pure torque (with unrestricted warping) produces no stresses in the corner flanges. Due to restricted warping at the root end, however, there will also be at each end a group of constraint forces (Fig. 8). Every group of constraint forces must have zero resultant force and zero resultant bending moment in the vertical as well as in the horizontal plane; the four forces composing the group must therefore be numerically equal and antisymmetrically arranged (such a group has been called "bicouple" in the literature). Notice that the four forces are numerically equal even though the thickness and flange areas show no symmetry (this is

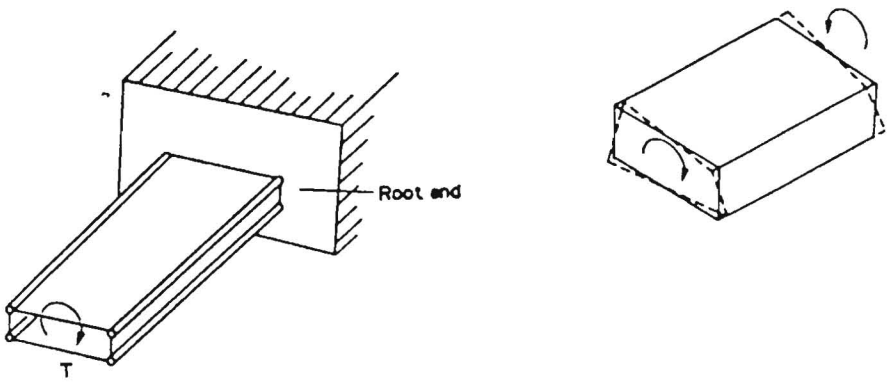

Fig. 7. Warping deformation. A restriction at the root end would produce constraint forces.

because the four-flange shell is rectangular). Let us denote the constraint forces by X_0. We shall first find the stresses in the shell caused by the system of X_0 forces. The shear flow in a given wall cannot vary along the length because such a variation could be effected only by intermediate bulkheads transferring torque from one pair of walls to the other pair, and no intermediate bulkheads are assumed to exist. The shear flow also cannot vary across the width because such a variation would imply the existence of axial stresses in the sheet, which are excluded by the assumption that the sheet carries only shear. The shear flow is therefore constant over any given wall, and as a consequence the forces in the flanges decrease linearly from their maximum values X_0 at the outboard end (root end) to zero at the inboard end (tip end) of the cell. The magnitudes of the two shear flows q_b^X and q_h^X can be determined by applying two equilibrium conditions. Since the system of X_0 forces exerts no resultant torque,

$$(q_b^X b)h + (q_h^X h)b = 0. \tag{33}$$

The condition of zero force $\Sigma X = 0$ applied to a corner flange (Fig. 8) gives

$$X_0 - q_h^X a + q_b^X a = 0. \tag{34}$$

The solution of the two equations gives

$$q_b^X = -\frac{X_0}{2a}; \quad \tau_b^X = -\frac{X_0}{2at_b}, \tag{35a}$$

$$q_h^X = \frac{X_0}{2a}; \quad \tau_h^X = \frac{X_0}{2at_h}. \tag{35b}$$

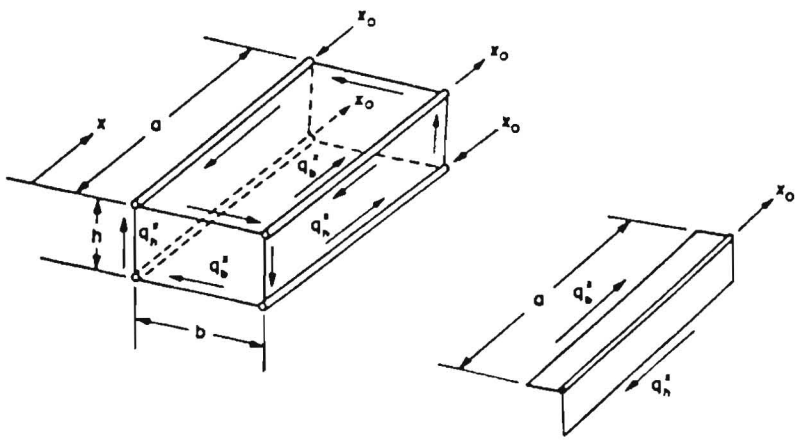

Fig. 8. Constraint forces.

Now we shall find the magnitude of X_0. The total stresses are the sum of those due to the torque T [eq. (32)] and those due to the system of forces X_0 [eq. (35)]:

$$\tau_b = \tau_b^T + \tau_b^X = \frac{T}{2bht_b} - \frac{X_0}{2at_b}, \tag{36a}$$

$$\tau_h = \tau_h^T + \tau_h^X = \frac{T}{2bht_h} + \frac{X_0}{2at_h}. \tag{36b}$$

Since we assume no warping, the ratio of the shear strains γ_b and γ_h given by (31) should equal the ratio of the shear stresses τ_b and τ_h [eq. (36)]:

$$\frac{\gamma_b}{\gamma_h} = \frac{\tau_b}{\tau_h} = \frac{h}{b}, \tag{37}$$

which gives

$$\frac{h}{b} = \frac{t_h(Ta - X_0 bh)}{t_b(Ta + X_0 bh)}. \tag{38}$$

Solving for X_0 we find

$$X_0 = \frac{Ta}{bh} \frac{\left(1 - \frac{h}{b}\frac{t_b}{t_h}\right)}{\left(\frac{h}{b}\frac{t_b}{t_h} + 1\right)}. \tag{39}$$

Notice that the force X_0 vanishes in the special case $h/b = t_h/t_b$, which means that in this case the warp would be zero (plane cross-sections remain plane) in an unrestricted shell.

Finally, there will be an axial stress in the flanges due to the force X_0 given by

$$\sigma_f = \frac{xX_0}{aA_f}, \tag{40}$$

the stress being compressive on two of the flanges and tensile on the other two. In the above expression A_f is the cross-sectional area of the flange and x is the distance from the tip end.

The compressive stress $\sigma_f(x)$ on the flange that carries the spot welds could cause local buckling of the segment between the spot welds. Although this stress varies linearly along the length, we can assume that the segment between the spot welds is acted upon by compressive forces of magnitude $\sigma_f A_f$, where σ_f is evaluated at the site midway between the spot welds. *Thus, we have again a case of buckling-assisted fatigue occurring in the case of torsion loading.*

Several other end conditions could be treated by similar arguments. For example, we could have a case of partial restriction at the end, i.e. the torque taken out by reactions, while the flange forces are transmitted by carry-through members of axial stiffness AE and so the warping due to torque is zero while the warping of the root end due to the flange forces is set by the stiffness of the carry-through members. If, on the other hand, warping is restricted at both ends then we have two systems of constraint end forces which, due to symmetry, are the same in magnitude and direction. The magnitude of each force would be half that given by eq. (39) and in this case the stress σ_f would vary linearly from compression at one end of the flange to tension of equal magnitude at the other. It should also be noted that the system of forces X_0, being self-balanced, affects primarily its immediate vicinity in accordance with Saint-Venant's principle of statically 'equipollent' systems. The magnitude of X_0, in turn, depends chiefly on the difference between the warps of the adjacent faces (a rigid root is heavily constrained because the foundation has zero warp). Such differences in warp can be caused otherwise by differences in torque or by differences in dimensions (local discontinuities).

RESULTS OF THE ANALYSIS

The objective of the analysis in the previous section was to find the cause of flange opening and buckling-assisted fatigue of spot welds in the case of torsional loading. The phenomenon had been observed in preliminary experiments of single hat box beam sections. Pending the completion

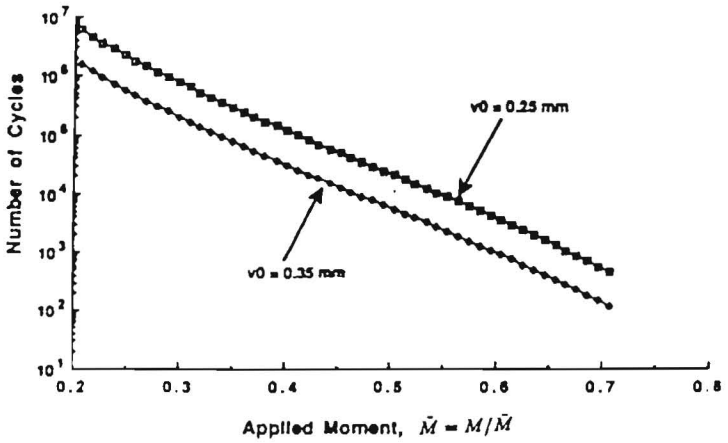

Fig. 9. Bending loading: number of cycles vs applied bending moment for initial imperfection $v_0 = 0.25$ and 0.35 mm (spot weld spacing $l = 75$ mm).

of a comprehensive test program and the acquisition of related experimental data we shall present in the following some analytical results on both torsion and bending that can provide useful trend information.

An example case was considered to illustrate the influence of the various parameters on the cyclic loading performance of the strucutre. A single hat section of length $a = 400$ mm and hat cross-section of height $h = 50$ mm and width $b = 100$ mm was chosen. The thickness of the steel sheet material was chosen to be uniformly $t = 1$ mm. The flange had a width of $w_f = 15$ mm and the spot welds had a diameter $d = 5$ mm. The material constants (steel) are: modulus of elasticity $E = 206{,}900\ \mathrm{MN/m^2}$ and Poisson's ratio $\nu = 0.32$. In the parametric studies the initial imperfection v_0 was in the range of 0.25–0.50 mm and the spot weld spacing was in the range of 40–80 mm. In the fatigue growth law $da/dN = A(\Delta J)^n$ and typical data for steel are $n = 2$ and $A = 1800\ \mathrm{MN^{-2}\,m^3}$.

Results of the analysis illustrate the sensitivity with respect to the spot weld spacing and with respect to the imperfection parameter (initial waviness). For the case of bending, Fig. 9 shows the number of fatigue cycles and Fig. 10 the J integral as a function of the applied bending moment for two values of the imperfection variable ($v_0 = 0.25$ mm and 0.35 mm) and spot weld spacing $l = 75$ mm. The applied load has been normalized with the quantity $\bar{M} = 2P_{cr}I_b/[tw_f(h + w_f)]$, where I_b is given by eq. (8) and P_{cr} is calculated at weld spacing $l_0 = 75$ mm.

The influence of the spot weld spacing is better illustrated in the case of torsion in Fig. 11, which shows the number of fatigue cycles, and in Fig. 12, which shows the J integral as a function of the spot weld spacing for two values of the imperfection variable ($v_0 = 0.25$ and 0.35 mm) and

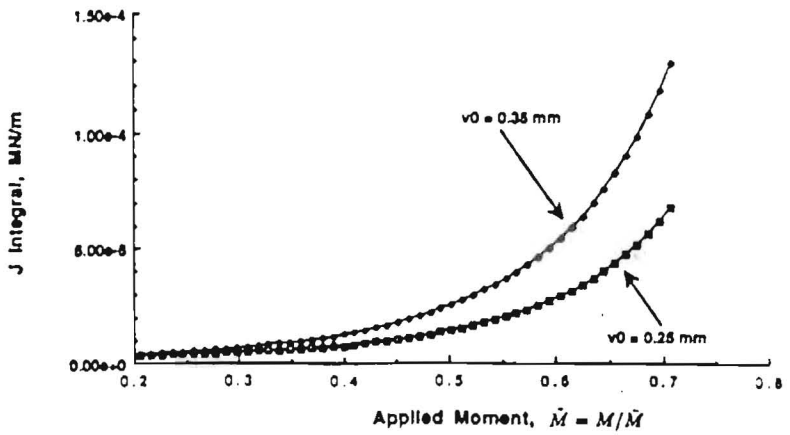

Fig. 10. Bending loading: J integral vs applied bending moment for initial imperfection $v_0 = 0.25$ and 0.35 mm (spot weld spacing $l = 75$ mm).

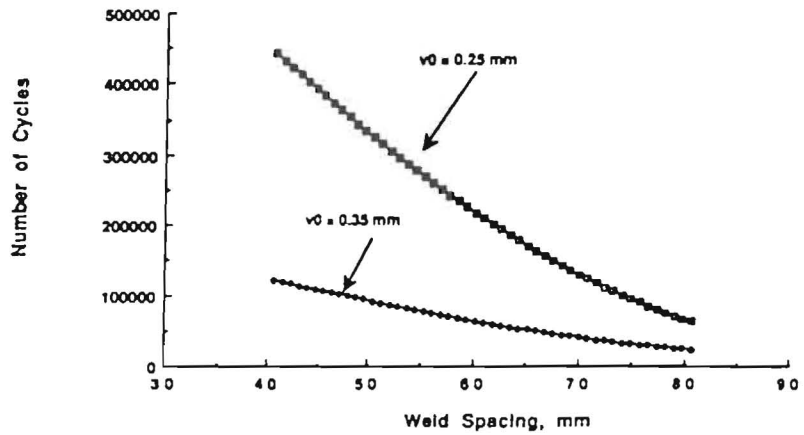

Fig. 11. Torsion loading: number of cycles vs spot weld spacing for initial imperfection $v_0 = 0.25$ and 0.35 mm (applied torque $\bar{T} = T/\bar{T} = 0.40$).

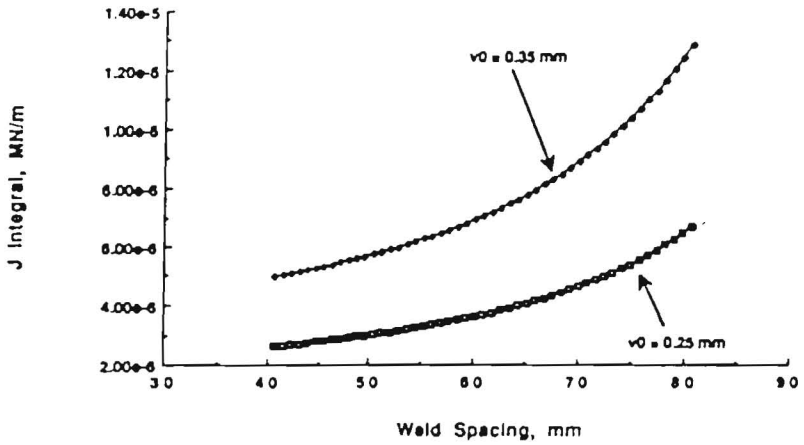

Fig. 12. Torsion loading: J integral vs spot weld spacing for initial imperfection $v_0 = 0.25$ and 0.35 mm (applied torque $\bar{T} = T/\bar{T} = 0.40$).

applied torque $\bar{T} = T/\bar{T} = 0.40$. The applied torsional loading has been normalized with the quantity $\bar{T} = P_{cr}(bh/a)[1 + (h/b)]/[1 - (h/b)]$, where P_{cr} is calculated at weld spacing $l_0 = 75$ mm.

It is seen that there is a value of the spot weld spacing above which further increase of the spacing significantly decreases the fatigue life. These results illustrate the basic freatures of the problem and could naturally be used in conjunction with more detailed analyses.

REFERENCES

[1] M. Oshima and H. Kitagawa, Buckling assisted fatigue of spot-welded box beam under bending. SAE (Society of Automotive Engineers) Paper 860605 (1986).
[2] P. C. Wang, H. T. Corten and F. V. Lawrence, A fatigue life prediction method for tensile-shear spot welds. SAE (Society of Automotive Engineers) Paper 850370 (1985).
[3] H. Abe, S. Kataoka and T. Satoh, Empirical formula for fatigue strength of single-welded joint specimens under tensile-shear repeated load. SAE (Society of Automotive Engineers) Paper 860606 (1986).
[4] J. A. Davidson, A review of the fatigue properties of welded sheet steel. SAE (Society of Automotive Engineers) Paper 830033 (1983).
[5] L. P. Pook, Fracture mechanics analysis of the fatigue behaviour of spot welds. *Int. J. Fracture* **11**, 173–175 (1975).
[6] S. P. Timoshenko and J. M. Gere, *Theory of Elastic Stability*. McGraw-Hill, New York (1961).
[7] J. R. Rice, A path independent integral and the approximate analysis of strain concentration by notches and cracks. *J. appl. Mech.* **35**, 379–386 (1968).
[8] P. C. Paris and F. Erdogan, A critical analysis of crack propagation laws. *J. bas. Engng* **85**, 528–533 (1963).
[9] P. Kuhn, *Stresses in Aircraft and Shell Structures*. McGraw-Hill, New York (1956).

(*Received* 30 *April* 1991)